

Effect of Warm Laser Shock Peening on Microstructure and Properties of GH4169 Superalloy

Taiyou Hu^{1,2}, Songxia Li³, Hongchao Qiao^{1,a}, Ying Lu¹, Boyu Sun¹ and Jiajun Wu^{1,2}

¹ Shenyang Institute of Automation Chinese Academy of Sciences, Liaoning, Shenyang 110016, China;

² University of Chinese Academy of Sciences, Beijing 100049, China;

³ Northeastern University, Liaoning, Shenyang 110004, China

*Corresponding author: ^a Hongchao Qiao: hcqiao@sia.cn

Abstract. In order to explore the effect of warm laser shock peening (WLSP) on the GH4169 superalloy, the microhardness, residual stress, and microstructure of the samples are compared and analyzed by laser shock peening (LSP) at 24 °C and WLSP at 200 °C, 250 °C, and 300 °C. The results show that the microhardness level and hardened layer thickness increase gradually with the increase of process temperature. Compared with LSP (24 °C), WLSP (300 °C) increased the maximum microhardness of the sample by 13.0% and the depth of hardened layer increased by 25.0% ; The influence of process temperature has little effect on the residual stress level, and the residual stress difference of the samples after LSP (24 °C) and WLSP (200 °C, 250 °C, 300 °C) are within 40MPa; Compared with the microstructure of the original sample, the dislocation density of the samples after LSP and WLSP increased significantly, compared with LSP (24 °C), the number of slip line projections after WLSP (300 °C) is more, the size is larger, and there are a lot of dislocations tangled around the precipitates. This study shows that WLSP has a better strengthening effect than LSP.

1. INTRODUCTION

High-temperature alloys are called superalloys in countries such as Britain and the United States. They are the main materials used for high-temperature core components in modern aero-engines, marine gas turbines and rocket engine power equipment [1]. According to statistics, the use of superalloys materials in modern aviation turbofan engines accounts for 40% to 60% of the entire engine [2]. Therefore, research and development of superalloys have significant scientific research and production value.

GH4169 is a superalloy developed by China in the 1960s. It belongs to precipitation hardening nickel-base superalloy, which has a high yield strength, tensile strength and plasticity below 650°C, and it also has good corrosion resistance, radiation resistance, thermal processing and welding performance. It is widely used in aviation, aerospace, nuclear energy, petrochemical, and other fields. And it is also one of the largest superalloys currently produced in China [3-5].

Laser Shock Peening (LSP) is a new type of surface enhancement technology. It introduces residual compressive stress on the surface of metallic materials through high-energy laser-induced shock waves, which can suppress the initiation and development of fatigue cracks, thereby significantly improving the fatigue resistance, corrosion resistance and wear resistance of metal



materials [8-12]. However, the microstructure formed by LSP is in a thermodynamically metastable state. Residual compressive stress relaxation and material degradation are very likely to occur under high-temperature conditions, which limits the application of LSP technology in high-temperature service environments. In order to improve the high-temperature stability of LSP, researchers at Purdue University [13-14] proposed the concept of Warm Laser Shock Peening (WLSP) in 2010. At present, the team has conducted partial research on WLSP, but mainly concentrates on low-temperature alloy materials, while domestic research is mainly focused on room-temperature LSP and less research on WLSP. In this experiment, GH4169 superalloy materials are subjected to WLSP at different process temperatures. The changes in surface microhardness, residual stress and microstructure are compared and analyzed. The effects of WLSP on the microstructure and properties of GH4169 superalloy materials are discussed.

2. EXPERIMENTAL PROCESS

2.1 Experimental materials and process parameters

The GH4169 nickel base alloy was selected as the experimental material, and its chemical composition is shown in Table 1. The block-shaped forged substrate was processed into the samples having a size of 20 mm×20 mm and a thickness of 2 mm using a wire cutter. The surface of all samples to be machined first was polished step by step through 100#~1000# SiC sandpaper, and then polished with a polishing agent having a particle diameter of 0.5 mm on a metallographic sample polishing machine.

Table 1. Chemical composition of GH4169 alloy (mass fraction, %)

Ni	Cr	C	Mn	Si	S	P	Mo
51.58	18.36	0.036	0.093	0.18	0.002	0.005	2.96
Al	Ti	B	Nb	Co	Cu	Fe	
0.56	0.99	0.003	5.03	0.02	0.02	bal	

High-performance Nd: YAG nanosecond pulsed laser with a wavelength of 1064nm is used to perform WLSP processing on the samples. The absorber layer is 100 μm thick aluminum foil, the constrained layer is 3mm thick K9 optical glass, the laser energy is 5J, the pulse width is 14ns, the spot diameter is 2mm, and the overlap ratio is 50%. In the WLSP experiment, the samples were first heated to a predetermined temperature, and then LSP were performed according to the designated trajectory. The impact trajectory and WLSP processed sample morphology are shown in Figure 1.

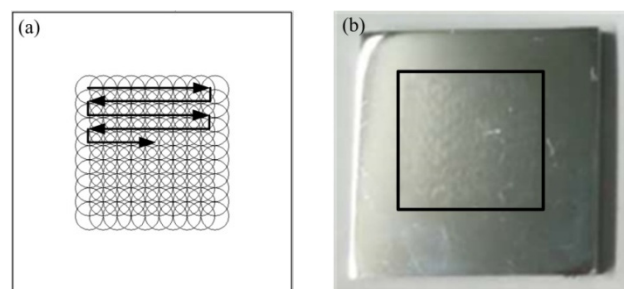


Figure 1. WLSP sample. (a) impact trajectory; (b) sample morphology after WLSP

As the only variable in the experiment, it is important to determine the appropriate WLSP temperature. WLSP combines the dual effects of LSP and dynamic strain aging (DSA). Therefore, the WLSP temperature must not only consider the temperature range during which the material generates DSA, but also take into account the characteristics of ultra-high strain rate of LSP. The "Qian-Xiao-Li model" proposed by Qian Kuangwu et al. [15] of Fuzhou University can be used to calculate the temperature range for DSA of alloys. The formulas are as follows:

$$T_1 = -Q_m / k \ln(a^2 / 12D_0) \quad (1)$$

$$T_2 = u_{\max} / k \ln(c_0 / c_s) \quad (2)$$

Where T_1 and T_2 are the upper and lower temperature limits for DSA, Q_m is the activation energy required for solute atoms to generate segregation, a is the lattice constant, D_0 is the diffusion constant, u_{\max} is the energy of the maximal interaction between solute atom and dislocations in the alloy, c_0 is the average concentration of solute elements in the alloy, c_s is the maximum concentration of solute atoms in the alloy at the junction of dislocations, which is related to temperature, k is the Boltzmann constant.

Based on the above model, the temperature range for DSA of the alloy is approximately 0.2~0.5 T_m (T_m is the melting point of the alloy), but the above conclusion is obtained under the condition of low strain rate, which is inconsistent with the strain rate of LSP at $10^6/s \sim 10^7/s$, and there is a certain deviation in the calculation results. In addition, Gopinath.K's [16] study has shown that there is a negative linear relationship between temperature and strain rate for DSA. Considering comprehensively, the WLSP experiment temperature range chooses 200~300°C.

2.2 Test Methods and Procedures

The LSP experiments were carried out at room temperature (24°C), 200°C, 250°C, and 300°C, respectively. The microhardness test in the depth direction, the surface residual stress test, and the observation of the microstructure of the surface were performed on the samples before and after strengthening.

2.2.1 Microhardness test

The indentation test was performed on the surface and in the depth direction of the samples using an HV-1000 micro-hardness tester manufactured by Beijing Times Peak Company. The measurement load is 100g and the retention time is 15 s. With the center of a shock pit as the starting point for the test, 0.25 mm increments in steps, three points are measured at each depth position and the arithmetic average is taken as the surface microhardness value of the sample. The samples were cut longitudinally along the center of the reinforced region using wire cutting, and microhardness tests were performed on the cross-section after grinding and polishing. With the reinforced surface as the starting point for the test, 100 μ m increments in steps, three points are measured at each depth position and the arithmetic average is taken as the microhardness value of the sample at that depth.

2.2.2 Residual Stress Test

The residual stress test was performed on the surface of the sample using a Proto-LXRD X-ray diffractometer manufactured by Canada Proto Company. The experiment uses the lateral fixation Ψ method, Ψ angle is selected as (0°, $\pm 5^\circ$, $\pm 15^\circ$, $\pm 20^\circ$, $\pm 30^\circ$, $\pm 36^\circ$), collimator diameter is 1mm, X-ray tube voltage is 25kV, tube current is 6mA, X-ray radiation selected $\text{CrK}\alpha$, diffraction crystal surface Ni{220}, 2θ angle scanning range is $150^\circ \sim 160^\circ$, scanning step distance is 0.02° , and scanning interval is 0.5s.

2.2.3 TEM observation

The microstructure of the samples before and after LSP were observed using transmission electron microscope (TECNAI20). First, the samples to be observed were cut into thin sheets having a thickness of about 300 μ m using a wire cutting machine, and then the sheets were polished to 30-50 μ m layer by layer with 100-1000# SiC waterproof sandpaper, and the sheets were punched into a small disc with a diameter of about 3mm by the punching machine. The punched small discs were subjected to double-spray electrolysis thinning, electrolyte is a 1:9 mixture of perchloric acid and ethanol, polishing voltage is 60 V and current is 50 mA. During the double-spray treatment, the dry ice was used to control

the electrolysis temperature within -25°C to -30°C . After the samples are perforated, cutting off the power, rinsing the sample and performing the transmission observation operation are then conducted.

3. RESULTS AND DISCUSSION

3.1 Microhardness

The distribution of microhardness along the depth direction of the WLSP samples is shown in Figure 2.

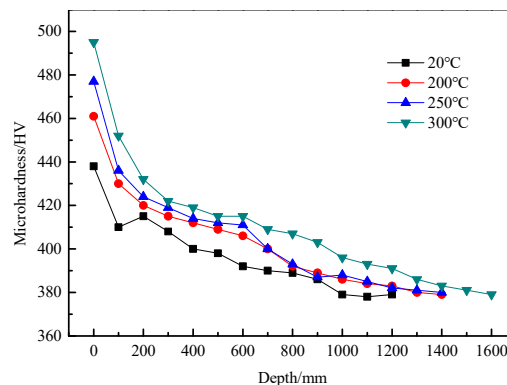


Figure 2. Distribution of microhardness along the depth direction

As shown in Figure 2, the microhardness and the depth of the hardened layer increase gradually with the increase of process temperature. Compared with LSP (24°C) samples, the maximum microhardness of WLSP samples at 200°C , 250°C , and 300°C increased by 5.3%, 8.9%, and 13.0%, respectively. When the WLSP temperature was 300°C , the maximum depth of the hardened layer was $1500\mu\text{m}$, an increase of 25.0% over LSP (24°C).

The increase in the microhardness level of the WLSP samples is attributed to changes in the grain size and flow stress of the material. On the one hand, the energy of the solute atoms in the alloy increases with the substrate temperature increases, and when the activation energy is large enough, the solute atoms will migrate and accumulate on the dislocation line, which will cause pinning effect on dislocations. The decrease of mobile dislocations causes the dislocation further multiplication, which promotes grain refinement [17]. According to the Hall-Petch formula [18]

$$H_v = H_{v0} + K_{Hv} d^{-1/2} \quad (3)$$

Where H_v and H_{v0} are respectively the microhardness of the treated sample and the microhardness value of the original matrix, K_{Hv} is the Hall-Petch constant, and d is the grain size.

From the formula (3), it can be seen that the further reduction of the grain size can obtain a greater microhardness. On the other hand, the material softens in the high temperature environment, the flow stress decreases, and the material is more prone to plastic deformation. Laser-induced shock wave can be applied farther inside the material, thereby increasing the depth of the surface hardened layer.

3.2 Residual stress

The surface residual stress of WLSP samples at different process temperatures is shown in Figure 3.

As shown in Figure 3, the residual compressive stress of the samples increases first and then decreases as the process temperature increases. When the WLSP temperature is 200°C , the surface residual stress is -335MPa , which is slightly higher than -323MPa of LSP (24°C); when the WLSP temperature are 250°C and 300°C , the surface residual stress are -312MPa and -302MPa , respectively, which are slightly lower than LSP (24°C).

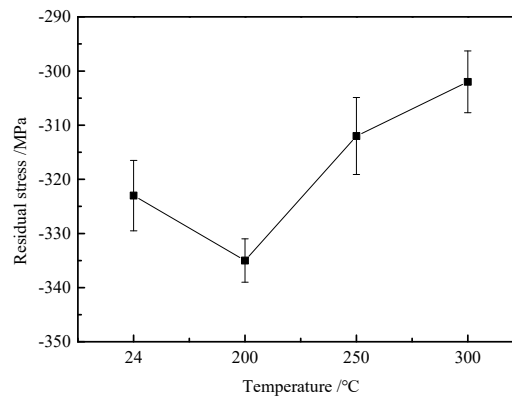


Figure 3. Effect of WLSP Process Temperature on Residual Stress of Sample Surface

From the above data, it can be seen that the residual stress difference of the WLSP samples are within 40 MPa at the process temperatures of 24°C, 200°C, 250°C, and 300°C, indicating that temperature in the interval has little effect on the residual stress of the sample. On the one hand, due to the material generate DSA in the heating environment, a large number of small precipitate particles precipitated from the supersaturated solid solution. At the same time, the dislocation density of the material rapidly increases under the action of laser-induced shock waves, the dislocations of the motion are hindered when the precipitates are encountered, dislocation pinning is formed, dislocation further value-added, increased density, causing increased residual stress. On the other hand, the samples are softened at high temperature, the elastic modulus of the material decreases, and the residual stress decreases. Under the comprehensive effect, the process temperature has little effect on the residual stress of the material surface.

3.3 Microstructure

The microstructure TEM image of the original sample of GH4169 superalloy is shown in Figure 4.

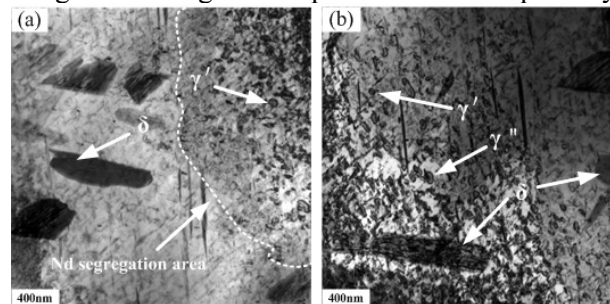


Figure 4. TEM image of microstructure of GH4169 superalloy original sample

As shown in Figure 4, a large number of disc-shaped γ'' strengthening phases and spherical γ' strengthening phases are dispersed in the white γ phase matrix, and a small number of dislocation structures are distributed around the strengthening phase. The lattice mismatch between γ'' phase and the matrix is large and has good coherence, which can significantly increase the strength of the alloy. The γ'' phase is the main strengthening phase. There are a small number of short rod-like or granular δ phases can be observed from Figure 4(a), and the δ phase is generally distributed at the grain boundaries to control grain growth. Nb segregation regions can also be observed from Figure 4(a), and a large number of γ' phases accumulate therein.

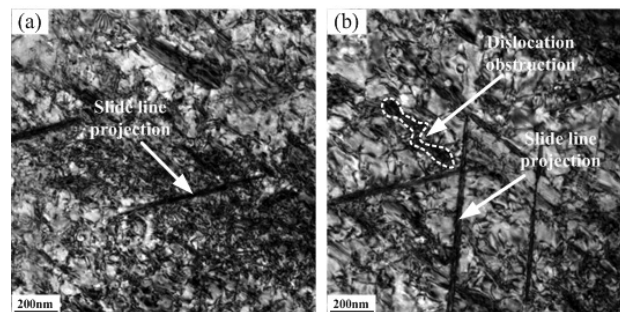


Figure 5. TEM image of GH4169 superalloy after LSP and WLSP. (a) LSP(24°C); (b) WLSP (300°C)

Figure 5 shows the surface microstructure TEM images of GH4169 superalloy after LSP (24°C) and WLSP (300°C). As can be observe Figure 5(a), the dislocation density of the sample after LSP (24°C) rapidly increases, and a small number of slide line projections are observed in the high density dislocation region. As can be observe in Figure 5(b), compared with the LSP (24°C) sample, the number of slide lines projected in the sample after WLSP (300°C) increased significantly, the projection size increased, and a large number of dislocations tangled around the strengthening phase.

The above phenomenon can be considered that, on the one hand, the material generates ultra-high strain rate plastic deformation under the action of a laser-induced shock wave, and the dislocation density of the material increases rapidly. On the other hand, the increase of substrate temperature leads to the enhancement of the activity of solute atoms, vacancies, and dislocations in the material. The material recovers at a low temperature and causes the concentration of vacancy and other point defects to decrease. In order to compensate for the local concentration imbalance caused by vacancies, dislocations generate slipping, climbing and other movements, resulting in an increase in the number of slip lines in the tissues. At the same time, a large number of fine precipitates precipitate generate DSA, When dislocations in motion encounter fine precipitates or diffusely distributed δ phases, MC carbides, γ'' , and γ' phases in the matrix, dislocations will pin up at these locations, forming pinning of dislocations.

4. CONCLUSION

With the increase of the temperature of the WLSP (200°C, 250°C, 300°C), the microhardness and the depth of the hardened layer increase gradually. Compared with the LSP (24°C) sample, the maximum microhardness of the sample after the WLSP (300°C) increased by 13.0 %, the depth of the hardened layer in sample eased by 25.0%, which is due to grain refinement and the reduction of material flow stress.

When the process temperature are 24°C, 200°C, 250°C and 300°C, the residual stress on the samples surface are -323MPa, -335MPa, -312MPa, and -302MPa, respectively, and the residual stress difference are within 40Mpa, which indicates that the process temperature has little effect on the residual stress of the sample.

Compared with the original sample, the dislocation density of the samples after LSP and WLSP have been significantly improved. Compared with LSP (24°C) sample, the number of slide lines in the sample after WLSP (300°C) is more and the size is larger. Under the double action of shock wave and DSA, a large number of dislocations tangled around the precipitates, forming a close pinning of dislocations.

WLSP combines the dual advantages of LSP and DSA. Compared with LSP samples, WLSP samples have a higher surface hardening level, which enhances the ability of the material surface to resist the destruction of hard objects. The material generates DSA, and a large number of small and fine precipitates are precipitated from the supersaturated solid solution and the dislocations are pinned, thereby improving the stability of the material. Therefore, WLSP has better strengthening effect than LSP.

References

- [1] Sims C T. Superalloys high-temperature materials for aerospace and industrial power [M]. New York: John Wiley & Sons, Inc. 1987, 1-10.
- [2] Ma K M, Bai B R, Wang H W. Aeronautical materials and applications[M]. Xian : Northwestern University Press, 2008: 177-187.
- [3] Xie X S, Dong J X, Fu S H, et al. Research and development of γ'' and γ' strengthened Ni-Fe base superalloy GH4169[J]. Acta Metallurgica Sinica, 2010, 46(11): 1289-1302.
- [4] Zhuang J Y. Deformation high temperature alloy GH4169[M]. Beijing: Metallurgical Industry Press, 2006: 1-60.
- [5] Huang Q Y, Li H H. Superalloy[M]. Beijing: Metallurgical Industry Press, 2000: 29-33.
- [6] Gong R Y. Research of microstructure evolution law and hot plastic deformation behavior for GH4169 alloy[D]. Shenyang: Northeastern University, 2014.
- [7] Loria E A. The Status and Prospects of Alloy 718[J]. JOM, 1988, 40(7): 36-41.
- [8] Lu Y, Zhao J J, Qiao H C, et al. Effects of Laser Peening on Micro-Structure Distributions and Deformation Microstructure of TiAl[J]. Acta Optica Sinica, 2014, 34(13): 269-274.
- [9] Caralapatti V K, Narayanswamy S. Analyzing the effect of high repetition laser shock peening on dynamic corrosion rate of magnesium [J]. Optics & Laser Technology, 2017, 93: 165-174.
- [10] Sealy M P, Guo Y B, Caslaru R C, et al. Fatigue performance of biodegradable magnesium-calcium alloy processed by laser shock peening for orthopedic implants [J]. International Journal of Fatigue, 2016, 82: 428-436.
- [11] Yang X W, Zhou J Z, Sheng J, et al. Microstructure evolution and surface strengthening mechanism of TC6 titanium alloy by laser peening[J]. Acta Optica Sinica, 2017, 37(9): 131-138.
- [12] Qiao H C, Zhao Y X, Zhao J B, et al. Effect of laser peening on microstructure and properties of TiAl alloy[J]. Optics and Precision Engineering, 2014, 22(07): 1766-1773.
- [13] Liao Y, Ye C, Kim B J, et al. Nucleation of highly dense nanoscale precipitates based on warm laser shock peening[J]. Journal of Applied Physics, 2010, 108(6): 1345.
- [14] Ye C, Suslov S, Kim B J, et al. Fatigue performance improvement in AISI 4140 steel by dynamic strain aging and dynamic precipitation during warm laser shock peening[J]. Acta Materialia, 2011, 59(3): 1014-1025.
- [15] Qian K W, Li X Q, Xiao L G, et al. Dynamic strain aging in metals and alloys[J]. Journal of Fuzhou University (Natural Science Edition), 2001, 29(6): 8-23.
- [16] Gopinath K, Gogia A K, Kamat S V, et al. Dynamic strain ageing in Ni-base superalloy 720Li [J]. Acta Materialia, 2009, 57(4): 1243-1253.
- [17] Zhou J J, Han Y H, Huang S, et al. Effect of different processing temperature on residual stress and nano-hardness of warm laser peened IN718 superalloy[J]. Chinese laser, 2015(7): 77-84.
- [18] Luong H, Hill M R. The effects of laser peening on high-cycle fatigue in 7085-T7651 aluminum alloy[J]. Materials Science & Engineering A, 2008, 477(1-2): 208-216.